

Electron transfer beyond the static picture: A TDDFT/TD-ZINDO study of a pentacene dimer

Randa Reslan,¹ Kenneth Lopata,² Christopher Arntsen,¹ Niranjan Govind,² and Daniel Neuhauser^{1,a)}

¹*Department of Chemistry and Biochemistry, University of California, Los Angeles, California 90095-1569, USA*

²*William R. Wiley Environmental Molecular Sciences Laboratory, Pacific Northwest National Laboratory, Richland, Washington 99352, USA*

(Received 19 February 2012; accepted 25 May 2012; published online 13 July 2012)

We use time-dependent density functional theory and time-dependent ZINDO (a semi-empirical method) to study transfer of an extra electron between a pair of pentacene molecules. A measure of the electronic transfer integral is computed in a dynamic picture via the vertical excitation energy from a delocalized anionic ground state. With increasing dimer separation, this dynamical measurement of charge transfer is shown to be significantly larger than the commonly used static approximation (i.e., LUMO+1–LUMO of the neutral dimer, or HOMO–LUMO of the charged dimer), up to an order of magnitude higher at 6 Å. These results offer a word of caution for calculations involving large separations, as in organic photovoltaics, where care must be taken when using a static picture to model charge transfer. © 2012 American Institute of Physics. [<http://dx.doi.org/10.1063/1.4729047>]

I. INTRODUCTION

Accurately computing electron transfer rates and probabilities is crucial for understanding a wide range of devices and effects, including many types of chemical reactions,^{1,2} solar cells,^{3,4} nanoelectronics,⁵ and molecular electronics.^{6–9} For example, in fullerene-based organic photovoltaics (OPVs), after photo-excitation of the light harvesting polymer, a charge-separated electron is first transferred to a nearby fullerene molecule, then subsequently shuttled to the electrode via a series of “hops” from one fullerene to another adjacent one. The success of an OPV often hinges on how readily electrons can be shunted from polymer to electrode without recombination with a hole. In general, this is a function of both the device morphology and also the electron transfer probability between two fullerene molecules. Increasing device efficiencies by optimizing transfer between fullerene pairs (e.g., via functionalization) thus offers a tantalizing opportunity. Unfortunately, predictive calculations of transfer probabilities are often elusive as electron transfer in these systems is a complicated process involving coupling between electronic and nuclear motion, in addition to the coupling with environment.

Electron transfer calculations on model systems and simple analogues offer a path forward. There has been much recent progress in modeling electron transfer between isolated molecules. The electron transfer reaction $A^-B^- \rightarrow AB^-$ is well established in principle using Marcus theory (for overview see Ref. 10), where the transfer is computed in the non-adiabatic regime – i.e., weak electronic coupling the donor and acceptor means that inter-conversion between from the donor to the acceptor diabatic potential energy surface can be computed semi-classically. Here, two

potential surfaces (reactants and products) are required as functions of molecular coordinates, and the transfer probability is computed from three main ingredients: ΔG^0 , the free energy difference between the two states; λ , the energy required to reorganize the system, possibly including a solvent shell, from initial to final state without actually transferring charge; and J , the electronic coupling between the initial and final states. While any number of theoretical approaches can be used within the Marcus framework (e.g., from semi-empirical to correlated methods), density functional theory (DFT) has been the most popular recently, due to good accuracy and modest computational cost.^{7,9,11–14}

For DFT, the main challenge lies in determining proper initial and final states in the transfer integral J in the Marcus formalism

$$J = |\langle \psi_F | H | \psi_I \rangle|^2,$$

where $|\psi_I\rangle$ and $|\psi_F\rangle$ are the initial and the final states, and H is the electronic coupling Hamiltonian (for more details, see review by Hsu¹⁵). Although at first glance this is straightforward, extreme care must be taken in choosing these states to avoid non-physical effects. For example, if one picks $|\psi_I\rangle = A^-B$ and $|\psi_F\rangle = AB^-$ the resulting dynamics could be dominated by electronic relaxation rather than charge transfer.

This issue of correct choice of initial and final states can be bypassed by simply comparing the LUMO and LUMO+1 of the neutral pair, which also gives a rough measure of the coupling (i.e., the larger the splitting the less the transfer probability). The picture, however, is only qualitative as in reality the transfer involves the coupling of a negatively charged molecule with a neutral one; this often consists of a significantly perturbed electronic structure from the neutral case.

For predictive calculations, however, the transfer integral J must be computed as accurately as possible, with proper

^{a)}E-mail: dxn@chem.ucla.edu.

choice of $|\psi_I\rangle$ and $|\psi_F\rangle$. To this end, we recently presented a new approach to electron transfer calculations named (time-dependent split) TD-split, where the transfer integral is calculated using the vertical excitation energy of a negatively charged dimer from a fully delocalized ground state;¹⁶ this excitation energy can be computed using virtually any time-dependent method. A related method is generalized Mulliken-Hush (GMH), which computes the coupling using the vertical excitation energy and transition dipole moment between two charge-localized states.¹⁷ In TD-split the nuclear degrees of freedom are frozen, the “reaction coordinate” is the degree of charge localization, and the resulting transfer integrals are associated with the rate of electron transfer for particular system geometry. This is contrast to traditional Marcus-type calculations, which includes the effect of the vibrational degree of freedom.

Marcus theory gives essentially the exact result (in the non-adiabatic limit) when the electronic transfer integrals are known. For large-scale systems, where the transfer integrals are almost always calculated by DFT, Hartree-Fock (HF), or Hartree-Fock (HF) or semi-empirical methods, most of the electronic degrees of freedom are frozen in the calculation. Put differently, the possibly crucial effect of the other electrons on the transfer is neglected in such single-particle static calculations, and TD-split corrects this omission. Therefore, in the non-adiabatic limit the result of TD-split can be viewed as the transfer integral in Marcus theory; when the distortion is weak and the vibrational degrees of freedom do not contribute, TD-split directly yields the transfer rate.

As a first step towards modeling charge transfer in OPVs, in this paper we use TD-split in conjunction with time-dependent density functional theory (TDDFT) and time-dependent ZINDO¹⁸ to study electron transfer across a pentacene dimer consisting of two planar stacked pentacene molecules with an intermolecular separation ranging from 3.5 Å to 6.0 Å (see Fig. 2). The rest of the paper is structured as follows: In Sec. II we briefly review the approach and discuss computational details, in Sec. III we present calculations on a pentacene dimer model system, and in Sec. IV we summarize the results and offer some outlooks on future directions.

II. METHODOLOGY

A. Static splitting

In this section, we briefly discuss both the TD-split (dynamic) and static approaches to computing the Marcus coupling term J . In the static picture, one assumes that the charge distribution for the neutral combination is not perturbed (dynamically or statically) by adding an extra electron. If that assumption is correct, the difference in energy between the LUMO+1 and LUMO for the neutral pair AB is equivalent to the Marcus factor for identical dimers with delocalized orbitals. Transition requires that the LUMO and LUMO+1 are delocalized over both fragments, otherwise the splitting will be high but there will be no transition; this effect is easily included with an additional weight term which measures the delocalization of the LUMO and LUMO+1.

B. Dynamic splitting

In the dynamic picture (TD-split), rather than use the LUMO+1–LUMO of the neutral system to compute the splitting (and thus the charge transfer rate), we instead use the vertical excitation energy (VEE) of the -1 charged dimer from a delocalized ground state, where the extra electron is equally shared between the two fragments. In a Marcus-like picture, this delocalized ground state is akin to an electronic “transition state” for the transferred electron; i.e., the intermediate situation between the charge on one fragment and the charge on the other, and the VEE is thus the electronic coupling between the two diabatic surfaces. Since the nuclear geometries are fixed, this does not correspond to the Marcus intermediate state, but rather to the halfway point in the electron transfer for the given geometry. By using the VEE of the -1 charged dimer from its delocalized ground state, you have carefully chosen the initial and final states in the transfer integral J to exclude non-physical re-arrangement of the electrons due to localization on one fragment or the other. In contrast, if you instead compute the transfer starting from a system with the extra electron localized on one fragment you will have added an indeterminate amount of energy; the calculation will thus give non-physical results since the localized charge perturbs the electronic density on the other fragment, and the resulting dynamics from this initial state will be dominated by electronic relaxation rather than transfer. An alternate approach is to use an isolating potential to create initial states with well-defined energies.¹⁹ When the vibrational degrees of freedom are weakly coupled, TD-split corresponds directly to the transfer rate. Note that when the system is not completely symmetric, the rate of transfer can still be obtained using the TD-split approach from a flux-flux time-dependent calculation which starts with the system in its ground anionic state (delocalized to a certain extent, depending on the degree of asymmetry) and then propagates the fluxes.¹⁶ The flux–flux result is the equivalent of the $|H_{AB}|^2$ term in Marcus theory.

Schematically, the TD-split approach can be expressed as

$$\delta A \equiv \langle \Psi(t) | A | \Psi(t) \rangle,$$

where $|\Psi(t)\rangle$ is a perturbed ground state for the entire charged system (including donor, acceptor, and the extra delocalized electron), and A is the perturbation operator. The time-dependent dynamics are thus directly associated with transport since the added charge is delocalized. In this method, the initial state is the ground static density matrix for the entire (donor and acceptor) charged system. A time-dependent excitation is applied and the response to this excitation is a measure of electron transfer rate. As formulated, this method is linear-response in nature. This type of calculation is “dynamic” in the sense that it goes beyond simply using the static eigenvalues of the single-particle Hamiltonian and instead accounts for electronic structure changes during the excitation. For example, in TDDFT this corresponds to correcting the static Kohn-Sham DFT eigenvalue differences with the electron-hole response. As will be shown later, these effects are crucial for properly capturing the separation dependence of the charge transfer.

C. Computational details

Both the static and dynamic approaches are flexible, as the orbital energies (LUMO, LUMO+1) and the vertical excitation energies can be computed via any number of static and time-dependent approaches, such as coupled cluster (e.g., equation of motion coupled cluster^{20,21}), linear-response^{22,23} or real-time TDDFT,^{24–28} or time-dependent semi-empirical methods.^{18,29} In this paper, we use DFT and ZINDO to compute the static splitting and VEEs of a -1 charged pentacene dimer. All DFT/TDDFT calculations were performed with atom-centered Gaussian basis sets using a development version of the NWChem software package.^{30,31} Since these methods are commonplace, we omit the details.

The ZINDO and TD-ZINDO results were obtained by using a modified version of ZINDO-MN package.³² In a nutshell, in ZINDO only the valence electrons are treated, which is done via semi-empirical one-body (i.e., nuclear and core) parameters h_{ij} and two-body interaction parameters v_{ijkl} , which are fit to experimental data,

$$F_{ij} = h_{ij} + \sum_{kl} v_{ijkl} P_{ij},$$

where P is the density matrix in the atomic orbital basis. The time-dependent response is computed using explicit time propagation via the von Neumann equation,

$$i \frac{\partial P'}{\partial t} = [F'(P'(t)), P'(t)],$$

where the prime denotes quantities in the molecular orbital (orthogonal) basis. The actual propagation was carried out using a linear-response von Neumann operator

$$LZ \equiv \frac{dZ}{dt} = -i \frac{[F'(P'_0 + \eta Z), P'_0 + \eta Z] - [F'(P'_0), P'_0]}{\eta},$$

where $Z(t) \equiv P'(t) - P'_0$ is the deviation of the MO density matrix from the initial state, and η is a small parameter ensuring linearity. $Z(t)$ is propagated from a dipole perturbed ground state $Z_0 = -i[D, P'_0]$ via a Chebyshev expansion, and the Fourier transform of the resulting time-dependent dipole moment yields the absorption spectrum, and thus the vertical excitation energies. For all TD-ZINDO simulations, the time step was 0.4 a.u. (0.01 fs) and the ZINDO parameters were taken to be as in the original ZINDO-MN package. For a more complete discussion of the TD-ZINDO approach see Ref. 18.

III. RESULTS

A. Convergence with basis set

The large separations in these systems can pose a serious problem for atom-centered basis sets, so as a first step we confirmed that the TDDFT and static splitting (LUMO+1–LUMO for the neutral dimer) results were all converged with basis.

Figure 1 shows the B3LYP TDDFT VEE for the negatively charged dimer, and the difference in energy between the LUMO and LUMO+1 for the neutral dimer for the 3-21G, 6-31G, 6-31++G, and POL1 basis sets. For shorter separations ($R < 4.5$ Å), both the static and TDDFT ener-

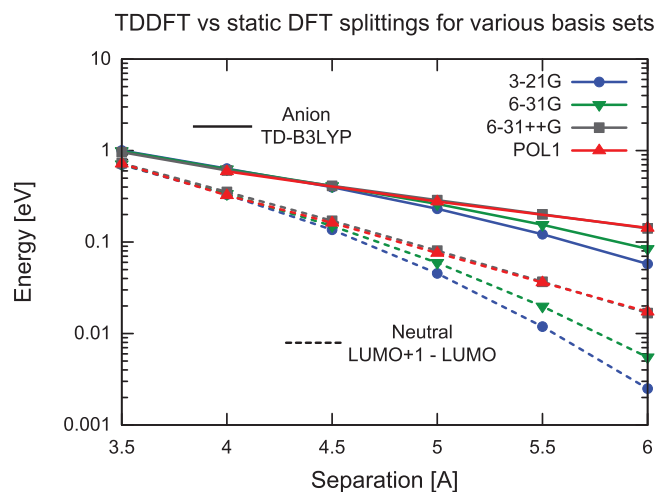


FIG. 1. Static B3LYP splitting (dashed) and TD-B3LYP energies (solid) for a range of basis sets. Larger separations require a basis set with diffuse functions (e.g., 6-31++G and POL1) to avoid non-physical super-exponential falloff.

gies are relatively insensitive to basis set, whereas there is a pronounced deviation from exponential behavior at larger separations for the 3-21G and 6-31G basis sets. The super-exponential falloff (nonlinear in log plot) is a non-physical consequence of the insufficient physical extent of the smaller basis sets. The POL1 basis, which is highly diffuse and optimized for response properties, retains the correct exponential falloff, as does the 6-31++G basis, which is a 6-31G basis with extra diffuse functions. The TDDFT VEEs are less sensitive to basis set than the static DFT LUMO+1–LUMO energies, since individual orbital energies are typically more sensitive to incomplete overlap due to finite basis. Given these results, we henceforth use the 6-31++G basis, which for our purposes yields effectively the same quality results as POL1 with significantly less computational effort (656 basis functions instead of 1308). In general, for calculations of this kind on extended systems, augmenting a small basis with a few diffuse functions offers an affordable way to capture charge transfer processes.

B. Static versus dynamic splittings

For the -1 charged system, the HOMO and LUMO are extended across the dimer, and the excitation corresponds to a symmetric \rightarrow antisymmetric flip for the dimer wavefunction (see Fig. 2). This is important because transitions between orbitals localized on individual fragments would result in an apparently large splitting, but with no electron transfer. This situation can be remedied somewhat by applying a “delocalizing” potential to the system to force a delocalized initial state but this was unnecessary for this symmetric system. The shapes of the neutral LUMO and LUMO+1 are qualitatively similar to the HOMO and LUMO of the negatively charged dimer (not shown), and since they are likewise extended, the difference in their energy is a fair measure of the static splitting.

Figure 3 shows the -1 charged dimer vertical excitation energies using a range of TDDFT exchange-correlation

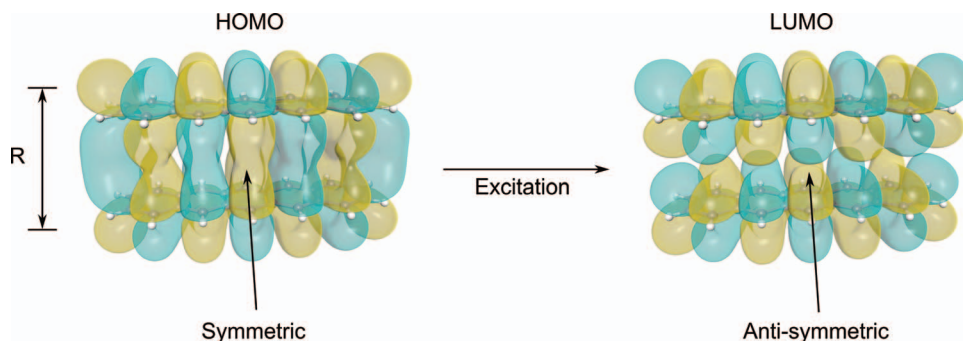


FIG. 2. Snapshots of the orbitals involved in the vertical excitation of the -1 charged dimer (5 \AA separation, PBE, 6-31++G basis). The excitation corresponds to a symmetric \rightarrow antisymmetric flip of the wavefunction.

functionals: local-density approximation (LDA) (slater exchange³³ and Vosko-Wilk-Nusair (VWN) correlation³⁴), Perdew-Burke-Ernzerhof (PBE) functional,³⁵ B3LYP.³⁶ The corresponding DFT neutral dimer LUMO+1–LUMO energies are shown for comparison. Overall, all TDDFT VEEs are quite insensitive to exchange-correlation functional; B3LYP is slightly red-shifted from LDA and PBE, but all have roughly the falloff rate (exponential decay constant 0.73 \AA^{-1}). For separations less than 4.5 \AA , there are intra-fragment excitations which are lower in energy than the HOMO \rightarrow LUMO excitation. These excitations are independent of separation, however, and with increasing R the HOMO \rightarrow LUMO transition is guaranteed to become the lowest excitation, since it decays exponentially with separation. The DFT neutral static splittings between the first two virtual states (LUMO+1 vs. LUMO) are likewise insensitive to the functional, but are both significantly shifted lower in energy than the TDDFT VEEs, and also decay much faster (1.5 \AA^{-1}). Figure 3 also shows the corresponding static and time-dependent ZINDO results. Since we are interested in the slope rather than absolute energies, they were scaled by 1.5 to facilitate comparison with the DFT results. The ZINDO

results are qualitatively similar to DFT, except for steeper exponential falloffs. Better tuning of the ZINDO coupling parameter might lead to better agreement with DFT.

Overall, these results suggest that the neutral static picture drastically underestimates the charge transfer rate, and the underestimation grows rapidly with increased separation. For example, whereas the static PBE energy is only 34% lower than the TD-PBE VEE at 3.5 \AA , it is a full order of magnitude smaller at 6 \AA . The reason for this is twofold: First, the static picture of orbital energy differences does not include re-arrangement of the electronic density during charge transfer; this is analogous to static DFT orbital energy differences versus TDDFT for traditional excitations. Second, the static picture assumes negligible perturbation of the electronic structure of the fragments upon adding an additional electron. Although the qualitative features of the orbitals (e.g., shape and ordering) are qualitatively unchanged by the additional electron, the orbital energetics are affected. For shorter separations, this effect is lessened since the dimer is more like a super-molecule. In a similar vein, the electronic structure of larger systems (e.g., fullerenes) is likewise less sensitive to extra electron.

In devices such as solar cells we are often interested in charge transfer across even larger length scales than these, so it is clear that a time-dependent approach is vital for even a qualitative description of the transfer. For example, it becomes impossible to use a static splitting-based calculation to correlate device morphology with charge transfer, since the static approach predicts far too fast a falloff with separation.

As a final check, we compared the neutral LUMO+1–LUMO splitting to the -1 charged HOMO–LUMO, as shown in Fig. 4. For pure DFT functionals (LDA, PBE), the two are virtually identical, which is consistent with the idea that the electronic structure of the dimer is negligibly affected by the addition of an extra electron. The anion splitting for the hybrid functional (B3LYP), however, is significantly overestimated, and falls off in an incorrect sub-exponential manner. For pure HF (not shown), this is even more pronounced. In a nutshell, HF is driving the system into an ionic-like state rather than a delocalized one, resulting in unphysical orbital energies; this failure of HF to describe anions is well-known. It is not surprising that B3LYP shows this behavior because it contains 20% HF. ZINDO, which is a HF-type method (albeit with modified interaction terms), also suffers from this problem.

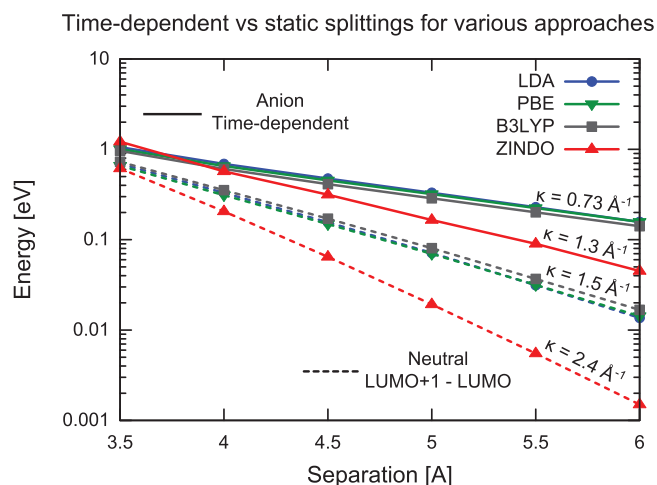


FIG. 3. Static DFT/ZINDO splitting for the neutral dimer (dashed) and HOMO \rightarrow LUMO TDDFT/TD-ZINDO vertical excitation energies for the -1 charged dimer (solid); the corresponding exponential decay constants are shown above each curve. All DFT calculations used the 6-31++G basis set. The ZINDO results are scaled by 1.5 for easier comparison.

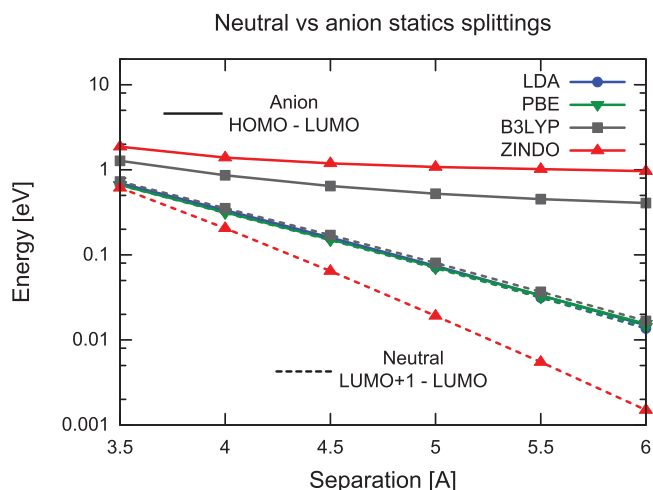


FIG. 4. Static splitting for the neutral and -1 charged dimer. The two agree well for pure DFT, but the anion is poorly described by B3LYP and ZINDO, due to the failure of HF to capture the delocalized ground state.

There are two things to note from these results: First, they confirm that dynamic (time-dependent) effects (e.g., electronic relaxation) are indeed important, and these calculations are not merely a measure of the anion static HOMO–LUMO splitting. Second, even though HF-based methods break down when describing the anionic orbital energies, the corresponding dynamics are still quite reasonable, i.e., the TD-B3LYP excitation energies are in excellent agreement with TD-LDA and TD-PBE, and TD-ZINDO is in reasonable agreement. Put another way, the response of the system is relatively insensitive to the poor ground state description.

IV. CONCLUSIONS

In summary, we computed the electronic couplings for a -1 charged pentacene dimer as a first step towards modeling electron transfer in organic photovoltaics. Two types of splitting were computed: the static DFT and ZINDO LUMO+1–LUMO of the neutral dimer, and the vertical excitation energy of the -1 charged dimer from a delocalized ground state, which was obtained via time-dependent methods (TDDFT and TD-ZINDO). The static picture consistently underestimates the splitting, and results in a far steeper exponential falloff than the dynamic splitting. As a consequence, while the static splitting offers a decent approximation to the transfer at short distances, with increasing separation it becomes ever more important to use the dynamic approach. These results have strong implications in systems like organic photovoltaics, where the LUMO+1–LUMO is a common rule of thumb for estimating charge transfer efficiency, since the addition of an extra electron on a fullerene is usually assumed to not significantly perturb the electronic structure. Care must be taken, however, as using the static approximation for large separations will drastically underestimate transfer probabilities, perhaps even by orders of magnitude in extreme cases. Future studies will address the accuracy of the static versus dynamic picture for charge transfer across fullerene pairs.

ACKNOWLEDGMENTS

A portion of the research was performed using the computing resources at Environmental Molecular Sciences Laboratory (EMSL), a national scientific user facility sponsored by the U.S. Department of Energy's (DOE) Office of Biological and Environmental Research and located at Pacific Northwest National Laboratory (PNNL). PNNL is operated for the DOE by the Battelle Memorial Institute under Contract No. DE-AC06-76RLO-1830. The work of R.R., C.A., and D.N. was supported as part of the Molecularly Engineered Energy Materials (MEEM), an EnergyFrontier Research Center funded by the U.S. Department of Energy, Office of Science, Office of Basic Energy Sciences under Award Number DE-SC0001342. K.L. acknowledges the William Wiley Postdoctoral Fellowship from Environmental Molecular Sciences Laboratory, and N.G. acknowledges the NWChem project for support.

- ¹K. V. Mikkelsen and M. A. Ratner, "Electron-tunneling in solid-state electron-transfer reactions," *Chem. Rev.* **87**, 113–153 (1987).
- ²W. Zhao, W. H. Ma, C. C. Chen, J. C. Zhao, and Z. G. Shuai, "Efficient degradation of toxic organic pollutants with $\text{Ni}_2\text{O}_3/\text{TiO}_2-x\text{B}_x$ under visible irradiation," *J. Am. Chem. Soc.* **126**, 4782–4783 (2004).
- ³B. O'Regan and M. Gratzel, "A low-cost, high-efficiency solar-cell based on dye-sensitized colloidal TiO_2 films," *Nature (London)* **353**, 737–740 (1991).
- ⁴W. Stier and O. V. Prezhdo, "Nonadiabatic molecular dynamics simulation of light-induced, electron transfer from an anchored molecular electron donor to a semiconductor acceptor," *J. Phys. Chem. B* **106**, 8047–8054 (2002).
- ⁵N. J. Tao, "Electron transport in molecular junctions," *Nat. Nanotechnol.* **1**, 173–181 (2006).
- ⁶G. L. Closs and J. R. Miller, "Intramolecular long-distance electron-transfer in organic-molecules," *Science* **240**, 440–447 (1988).
- ⁷J.-L. Brédas, D. Beljonne, V. Coropceanu, and J. Cornil, "Charge-transfer and energy-transfer processes in pi-conjugated oligomers and polymers: A molecular picture," *Chem. Rev.* **104**, 4971–5003 (2004).
- ⁸A. Nitzan and M. A. Ratner, "Electron transport in molecular wire junctions," *Science* **300**, 1384–1389 (2003).
- ⁹V. Lemaire, D. A. da Silva Filho, V. Coropceanu, M. Lehmann, Y. Geerts, J. Piris, M. G. Debije, A. M. van de Craats, K. Senthilkumar, L. D. A. Siebbeles, J. M. Warman, J.-L. Brédas, and J. Cornil, "Charge transport properties in discotic liquid crystals: A quantum-chemical insight into structure-property relationships," *J. Am. Chem. Soc.* **126**, 3271–3279 (2004).
- ¹⁰R. A. Marcus and N. Sutin, "Electron transfers in chemistry and biology," *Biochim. Biophys. Acta* **811**, 265–322 (1985).
- ¹¹Q. Wu and T. Van Voorhis, "Extracting electron transfer coupling elements from constrained density functional theory," *J. Chem. Phys.* **125**, 164105 (2006).
- ¹²T. Stein, L. Kronik, and R. Baer, "Reliable prediction of charge transfer excitations in molecular complexes using time-dependent density functional theory," *J. Am. Chem. Soc.* **131**, 2818 (2009).
- ¹³C. Liu, D. Walter, D. Neuhauser, and R. Baer, "Molecular recognition and conductance in crown ethers," *J. Am. Chem. Soc.* **125**, 13936–13937 (2003).
- ¹⁴H. N. Chen, M. A. Ratner, and G. C. Schatz, "Time-dependent theory of the rate of photo-induced electron transfer," *J. Phys. Chem. C* **115**, 18810–18821 (2011).
- ¹⁵C. P. Hsu, "The electronic couplings in electron transfer and excitation energy transfer," *Acc. Chem. Res.* **42**, 509–518 (2009).
- ¹⁶L. A. Bartell, R. Reslan, M. R. Wall, R. D. Kennedy, and D. Neuhauser, "Electron transfer with TD-split, a linear response time-dependent method," *Chem. Phys.* **391**, 62–68 (2011).
- ¹⁷R. J. Cave and M. D. Newton, "Generalization of the Mulliken-Hush treatment for the calculation of electron transfer matrix elements," *Chem. Phys. Lett.* **249**, 15–19 (1996).
- ¹⁸L. A. Bartell, M. R. Wall, and D. Neuhauser, "A time-dependent semiempirical approach to determining excited states," *J. Chem. Phys.* **132**, 234106 (2010).

- ¹⁹H. Eshuis and T. van Voorhis, "The influence of initial conditions on charge transfer dynamics," *Phys. Chem. Chem. Phys.* **11**, 10293–10298 (2009).
- ²⁰R. J. Bartlett and M. Musial, "Coupled-cluster theory in quantum chemistry," *Rev. Mod. Phys.* **79**, 291–352 (2007).
- ²¹K. Kowalski and P. Piecuch, "New coupled-cluster methods with singles, doubles, and noniterative triples for high accuracy calculations of excited electronic states," *J. Chem. Phys.* **120**, 1715–1738 (2004).
- ²²M. E. Casida, in *Recent Advances in Density Functional Methods*, edited by D. P. Chong (World Scientific Publishing, River Edge, NJ, 1995), Vol. 1, pp. 155–192.
- ²³S. Hirata and M. Head-Gordon, "Time-dependent density functional theory for radicals: An improved description of excited states with substantial double excitation character," *Chem. Phys. Lett.* **302**, 375–382 (1999).
- ²⁴C. L. Moss, C. M. Isborn, and X. S. Li, "Ehrenfest dynamics with a time-dependent density-functional-theory calculation of lifetimes and resonant widths of charge-transfer states of Li(+) near an aluminum cluster surface," *Phys. Rev. A* **80**, 024503 (2009).
- ²⁵K. Yabana and G. F. Bertsch, "Time-dependent local-density approximation in real time," *Phys. Rev. B* **54**, 4484–4487 (1996).
- ²⁶A. Castro, H. Appel, M. Oliveira, C. A. Rozzi, X. Andrade, F. Lorenzen, M. A. L. Marques, E. K. U. Gross, and A. Rubio, "Octopus: A tool for the application of time-dependent density functional theory," *Phys. Status Solidi B* **243**, 2465–2488 (2006).
- ²⁷K. Lopata and N. Govind, "Modeling Fast electron dynamics with real-time time-dependent density functional theory: Application to small molecules and chromophores," *J. Chem. Theory Comput.* **7**, 1344–1355 (2011).
- ²⁸R. Baer and D. Neuhauser, "Real-time linear response for time-dependent density-functional theory," *J. Chem. Phys.* **121**, 9803–9807 (2004).
- ²⁹J. D. Baker and M. C. Zerner, "Applications of the random phase approximation with the Indo/S Hamiltonian – Uv-Vis spectra of free base porphyrin," *Chem. Phys. Lett.* **175**, 192–196 (1990).
- ³⁰M. Valiev, E. J. Bylaska, N. Govind, K. Kowalski, T. P. Straatsma, H. J. J. Van Dam, D. Wang, J. Nieplocha, E. Apra, T. L. Windus, and W. de Jong, "NWChem: A comprehensive and scalable open-source solution for large scale molecular simulations," *Comput. Phys. Commun.* **181**, 1477–1489 (2010).
- ³¹See <http://www.nwchem-sw.org/> for NWChem.
- ³²M. C. Zerner, ZINDO-MN, version 2011 ed., Quantum Theory Project, University of Florida, Gainesville, FL; Department of Chemistry, University of Minnesota, Minneapolis, MN, 2011.
- ³³J. C. Slater and K. H. Johnson, "Self-consistent-field $X\alpha$ cluster method for polyatomic-molecules and solids," *Phys. Rev. B* **5**, 844 (1972).
- ³⁴S. H. Vosko, L. Wilk, and M. Nusair, "Accurate spin-dependent electron liquid correlation energies for local spin-density calculations – A critical analysis," *Can. J. Phys.* **58**, 1200–1211 (1980).
- ³⁵J. P. Perdew, K. Burke, and M. Ernzerhof, "Generalized gradient approximation made simple," *Phys. Rev. Lett.* **77**, 3865 (1996).
- ³⁶P. J. Stephens, F. J. Devlin, C. F. Chabalowski, and M. J. Frisch, "Ab-initio calculation of vibrational absorption and circular-dichroism spectra using density-functional force-fields," *J. Phys. Chem.* **98**, 11623–11627 (1994).